



Solid-state synthesis and magnetic properties of epitaxial FePd₃(0 0 1) films

V.G. Myagkov^{a,*}, V.S. Zhigalov^{a,b}, B.A. Belyaev^{a,b}, L.E. Bykova^{a,b}, L.A. Solovyov^c, G.N. Bondarenko^c

^a Kirensky Institute of Physics, SB RAS, 660036 Krasnoyarsk, Russia

^b Reshetnev Siberian State Aerospace University, 660014 Krasnoyarsk, Russia

^c Institute of Chemistry and Chemical Technology, SB RAS, 660049 Krasnoyarsk, Russia

ARTICLE INFO

Article history:

Received 7 September 2011

Received in revised form

24 November 2011

Available online 9 December 2011

Keywords:

Fe–Pd system

Thin film

Solid-state synthesis

Order–disorder transformation

Magnetic anisotropy

ABSTRACT

The solid-state synthesis of magnetically soft phase FePd₃ in epitaxial Pd(0 0 1)/Fe(0 0 1)/MgO(0 0 1) film systems was studied experimentally. The system had a Fe to Pd ratio of 1:3. An increase to 450 °C leads to the formation of three variants of ordered L1₀-FePd crystallites. At 500 °C, the solid-state reaction of unreacted Pd with L1₀-FePd crystallites initiates the growth of an ordered epitaxial L1₂-FePd₃(0 0 1) layer. When annealing at 650 °C, a gradual disordering is observed. The magnetic anisotropy ($K_1 = -2.0 \times 10^3$ erg/cm³) and the saturation magnetization ($M_S = 650$ emu/cm³) of the disordered FePd₃ phase were determined.

© 2011 Elsevier B.V. All rights reserved.

1. Introduction

Recently, Fe_xPd_{1-x} alloys have been intensively studied because of their unique magnetic and structural properties, which have promising practical applications. Iron-rich films with compositions near Fe₇₀Pd₃₀ exhibit features typical of bulk samples, such as superelasticity, magnetic shape memory effects [1], and martensitic transformations [2]. The most interesting of these are the L1₀-FePd films and nanoparticles of equiatomic composition. Characterized by their high anisotropy magnetic energies ($\sim 10^7$ erg/cm³) [3–12], they are considered to be promising media for high-density magnetic storage [3–12]. Many studies of the correlation between the perpendicular anisotropy and magnetization (M_S) and the structural properties of the L1₀-FePd thin films [3–7] and nanoparticles [8–10] have been performed. The formation of the L1₀ phase strongly depends on the annealing and deposition temperatures. In particular, after annealing at ~ 673 K, the L1₀-FePd phase was present in the Fe/Pd bilayers [5,12] multilayers [6] and electrodeposited Fe–Pd thin films [11]. The state diagram in the Pd-rich region contains the ferromagnetic Pd₃Fe phase with an ordered L1₂ structure. Recently, the L1₂ phase was found in nanoparticles formed by successive depositions of Pd and Fe onto a single-crystal NaCl(0 0 1) substrate kept between 560 and 570 K [8]. Currently, there is little data on the conditions necessary for the formation and ordering of the Pd₃Fe phase and its magnetic properties in bulk samples, thin films, and

nanoparticles. Studies of the solid-state reactions between elemental Fe and Pd reagents may yield important information on this formation and ordering during growth and annealing.

In this study, the solid-state synthesis of epitaxial Pd₃Fe(0 0 1) films on a MgO(0 0 1) surface was investigated. During the process of increasing the annealing temperature, Pd(0 0 1)/Fe(0 0 1)/MgO(0 0 1) samples were successively formed. They had Fe:Pd composition ratios of 1:3, ordered L1₀-FePd and L1₂-Pd₃Fe phases, and close initiation temperatures. We determined the magnetic characteristics of the Pd₃Fe(0 0 1) films, which are magnetically soft in both ordered and disordered states.

2. Samples preparation and experimental procedure

The initial Pd(0 0 1)/Fe(0 0 1) film structures were obtained by successive depositions of Fe and Pd layers onto a single-crystal MgO(0 0 1) substrate in a vacuum chamber at a pressure of 10^{-6} mbar. Before deposition, the substrates were outgassed at 570 K for 1 h. In the experiments, samples with atomic ratios of 1:3 (Fe:Pd) and a total thickness of 300 nm were used. The layers were deposited at temperatures between 220 and 250 °C. Fe(0 0 1) and Pd(0 0 1) were successively grown on the MgO(0 0 1) surface without solid-state reactions between the layers (Fig. 1a). In-plane hysteresis loops were taken using a vibrating sample magnetometer and a magneto-optic Kerr effect magnetometer. The four-fold in-plane magnetic anisotropy constants (K_4) of the samples were measured using a torque method with a maximum magnetic field of 18 kOe and ferromagnetic resonance (FMR). The FMR spectra were taken from local 0.8 mm² areas with an automated

* Corresponding author: Tel.: +7 3912 494681; fax: +7 3912 438923.
E-mail address: miagkov@iph.krasn.ru (V.G. Myagkov).

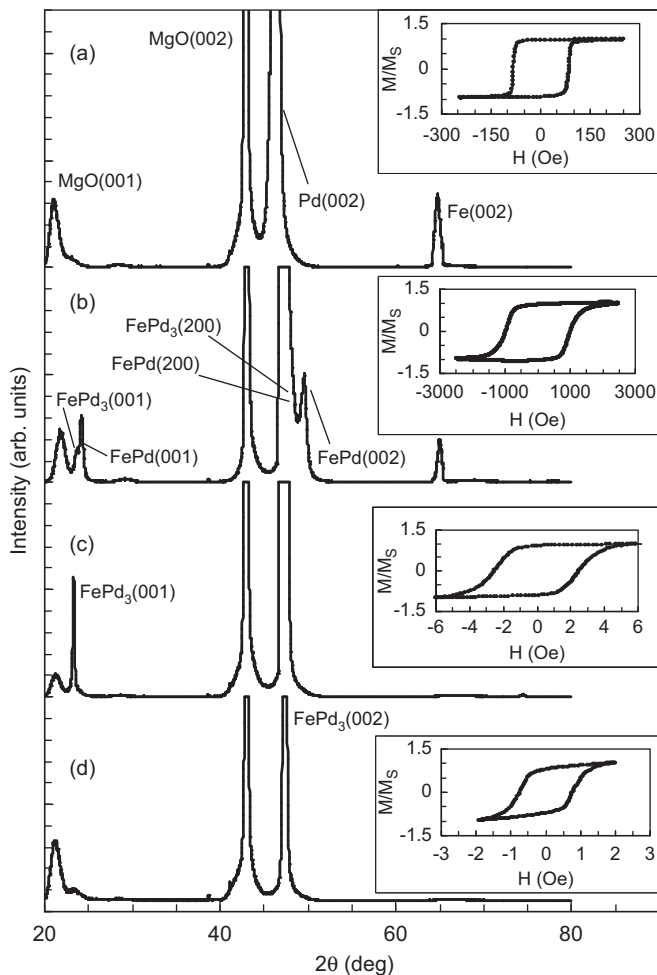


Fig. 1. XRD patterns of the 1:3 (Fe:Pd) Pd(001)/Fe(001)/MgO(001) film system and corresponding hysteresis loops measured along the easy axis: (a) initial sample and sample after annealing at (b) 450 °C, (c) 550 °C, and (d) 650 °C.

scanning spectrometer [13] at the pumping frequency $f=2.274$ GHz and a dc magnetic field scan in the film plane. Thicknesses of the Fe and Pd layers were determined using X-ray fluorescent analysis. The phases formed were identified using X-ray diffraction (XRD, $\text{CuK}\alpha$ radiation). The epitaxial film orientations were analyzed through asymmetrical XRD scans performed on a PANalytical X'Pert PRO diffractometer (Almelo, The Netherlands) with a PIXcel detector. The initial Pd(001)/Fe(001)/MgO(001) samples were thermally annealed at temperatures ranging from 300 to 650 °C in intervals of 50 °C and exposure times of 30 min at each temperature. All measurements were carried out at room temperature.

3. Results and discussion

The XRD patterns of the initial sample contained only Fe(002) and Pd(002) reflections (Fig. 1a), indicating the oriented growth of Pd(001)/Fe(001)/MgO(001). According to the XRD measurements, the growth of the Fe and Pd layers satisfies the Pd(001)[100] || Fe(001)[110] || MgO(001)[100] orientation relationship [12]. The torque curves show that the Fe(001) layer can be characterized through the fourfold anisotropy with easy axes directed along the [110] and $[1\bar{1}0]$ axes of the MgO(001) substrate. They had a constant of $K_4=5.0 \times 10^5$ erg/cm³ (for the volume of Fe layer), which coincides with the first constant of the magnetocrystallographic

anisotropy of bulk iron. The values of the coercivity ($H_C \sim 100$ Oe) and constant (K_4) and the orientation relationships were typical of Fe(001) films on MgO(001) obtained through other methods [14–16]. The subsequent deposition of the Pd(001) layer did not change the magnetic characteristics of the Fe(001) film.

Fig. 2 shows the dependence of the saturation magnetization (M_S) and K_4 (for the total volume of 3Pd:1Fe bilayer) on the annealing temperature. The values of M_S and K_4 remain constant for annealing temperatures up to 350 °C and exhibit changes in value after annealing at 400 °C. This indicates the initiation of the solid-state reaction between the Fe and Pd layers. The saturation magnetization becomes lower (Fig. 2b), the coercivity $H_C \sim 1000$ Oe increases by a factor of ~ 10 (Fig. 1b), and the in-plane fourfold anisotropy constant $K_4 \sim 3.5 \times 10^5$ erg/cm³ (Fig. 2a) increases by a factor of ~ 3 without a change in the direction of its easy axes. This indicates the formation of a highly anisotropic L1₀-FePd phase, which forms at ~ 400 °C in 1:1 (Fe:Pd) Fe(001)/Pd(001)/MgO(001) samples [12]. Further increases in K_4 after annealing at 450 °C are a consequence of the increasing volume of the L1₀-FePd phase in the sample (Fig. 2a). XRD study confirmed the formation of the ordered L1₀-FePd phase (Fig. 1b). At 450 °C, the Fe(002) reflection decreases considerably, and the (001) and (002) peaks of the ordered L1₀-FePd phase and the (100) peak of the ordered L1₂-FePd₃ phase appear. Note that the (002) peak of unreacted Pd conceals the (200) reflections of the L1₀-FePd and L1₂-FePd₃ phases. The large value of K_4 ($\sim 3.5 \times 10^5$ erg/cm³) and the occurrence of the (001), (002), and (200) reflections from L1₀-FePd after annealing at 450 °C suggest that the layer of reaction products contains three variants of crystallites of L1₀-FePd phase with three orthogonal axes parallel to the three main $\langle 100 \rangle$ axes of the MgO(001) plane induce a K_4 of $\sim 3.5 \times 10^5$ erg/cm³, which can be determined by the large value of the second constant of the magnetocrystallographic anisotropy ($K_2=(1.5 \pm 0.5) \times 10^6$ erg/cm³) of the L1₀-FePd phase [12]. The synthesis of the L1₀-FePd and

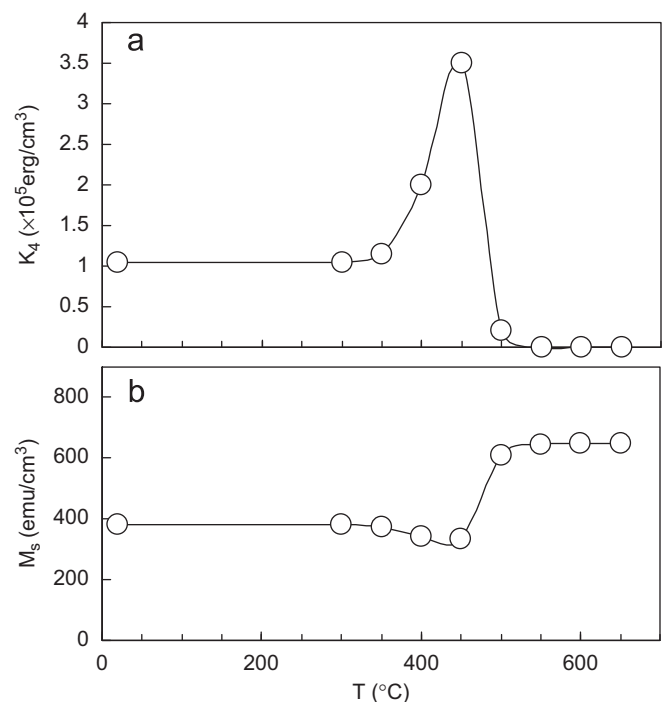


Fig. 2. Saturation magnetization (M_S) and the in-plane fourfold magnetic anisotropy constant (K_4) of the 1:3 (Fe:Pd) Pd(001)/Fe(001)/MgO(001) film system as a function of the annealing temperature.

L_{12} -FePd₃ phases for annealing temperatures up to 450 °C are similar for both 1:3 and 1:1 (Fe:Pd) samples.

At an annealing temperature of 500 °C, a solid-state reaction of the unreacted Pd layer with the L_{10} -FePd layer and the formation of the ordered L_{12} -FePd₃(0 0 1) phase with the lattice parameter $a=0.3841$ nm occurs. Using asymmetric XRD scans of the (1 1 3) reflections, the L_{12} -FePd₃(0 0 1)[1 0 0] || MgO(0 0 1)[1 0 0] epitaxial orientation relationship was identified (Fig. 3). The ordering degree parameter S of L_{12} -FePd₃ was derived from the occupancies of the Fe and Pd positions in the structure, which were determined using the full-profile XRD refinement. The value of S was determined after annealing at a temperature of 550 °C, at which only the L_{12} -FePd₃ phase was observed in the sample (Fig. 1c). The calculated estimate of $S=0.81 \pm 0.02$ indicates that a high degree of chemical ordering occurs under the nonequilibrium conditions of synthesis of the L_{12} -FePd₃ phase. Such samples had low coercivity values ($H_C \sim 2.0$ Oe (Fig. 1c)), fourfold anisotropy constants ($K_4 < 1 \times 10^4$ erg/cm³), and saturation magnetization ($M_S=650$ emu/cm³ (Fig. 2)). Annealing temperatures of 650 °C nearly eliminate the superstructural (1 0 0) reflection because of the disordering of the L_{12} -FePd₃ phase (Fig. 1d). The disordered FePd₃ phase maintained the same orientation relationship with the MgO(0 0 1) substrate, and the same value of saturation magnetization (Fig. 2b). However, the coercivity decreased somewhat: $H_C < 1.0$ Oe (Fig. 1d).

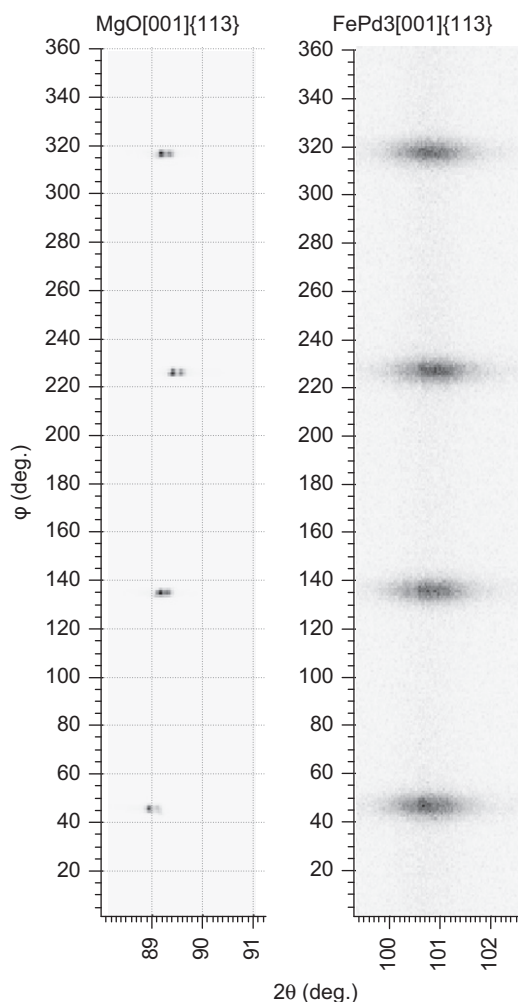


Fig. 3. The φ – 2θ asymmetric diffraction images for MgO substrate and FePd₃ film. These scans reveal the L_{12} -FePd₃(0 0 1)[1 0 0] || MgO(0 0 1)[1 0 0] epitaxial orientation relationship.

The first constant of the magnetocrystallographic anisotropy (K_1) was found using FMR measurements, which confirmed the magnetically soft nature of the FePd₃ films. Fig. 4 shows the angular dependence of resonance field H_r and linewidths ΔH for the disordered FePd₃ phase after annealing at 650 °C. The fourfold anisotropy with easy axes along the $\langle 1 1 0 \rangle$ directions of the FePd₃(0 0 1) film was observed in the angular dependence of both resonance field $H_r(\varphi)$ and linewidth $\Delta H(\varphi)$. The magnetic parameters calculated from the experimental data were $4\pi M_{eff}=8480$ Oe (M_{eff} is the effective saturation magnetization) and $2K_1/M_S \approx 5.6$ Oe ($2K_1/M_S$ is the fourfold anisotropy field). Also, there is uniaxial magnetic anisotropy that is insignificant in value. However, this component destroys the cubic symmetry of the angular dependence $H_r(\varphi)$ (Fig. 4a). Using the measured value $M_S=650$ emu/cm³ (Fig. 1b), the first constant of the magnetocrystallographic anisotropy $K_1=-2.0 \times 10^3$ erg/cm³ for the disordered FePd₃ phase was obtained. The value of K_1 is negative, which is similar to the case of Ni films, because the easy axes coincide with the $\langle 1 1 0 \rangle$ directions of FePd₃(0 0 1) (Fig. 4). These are the projections of the $\langle 1 1 1 \rangle$ directions onto the (0 0 1) surface.

A unique feature of solid-state reactions in thin-film bilayers and multilayers is the formation of only one phase (first phase) at the interface upon heating above the initiation temperature (T_0). Further increases in temperature lead to the formation of other phases (phase sequence) [17,18]. At present, there are no first-principles methods for obtaining the first phase, phase sequence, or their initiation temperatures for formation. As shown previously, the initiation temperature T_0 of the solid-state reaction in thin-film bilayers and multilayers coincides with the minimum temperature of the structural phase transformation in a given binary system [19–22]. In particular, the solid state reaction between Au and Cu begins at the minimum order–disorder temperature (240 °C) of the Au–Cu system with the formation of CuAuI and CuAuII superstructures [19]. The solid-state reactions in Co/Pt [20], Ni/Fe [21], Cu/Fe [22] bilayers start at

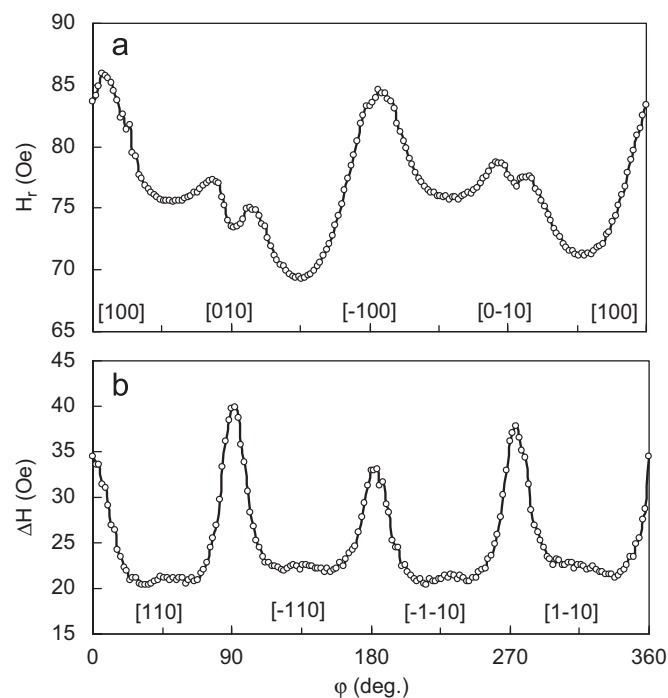


Fig. 4. In-plane angular dependence of the (a) resonance field H_r and (b) linewidth ΔH for the disordered FePd₃ sample after annealing at 650 °C. The calculated value of the resonance field yields $4\pi M_{eff}=8480$ Oe and a cubic anisotropy constant of $K_1=-2.0 \times 10^3$ erg/cm³.

temperatures of the order–disorder transition, eutectoid decomposition, respectively. These correspond to the minimum temperature of the structural phase transformation in the Co–Pt, Ni–Fe, Cu–Fe systems. Because the synthesis of the ordered L1₀-FePd and L1₂-FePd₃ phases is observed at temperatures above $T_0 \sim 400$ °C, we suggest that 400 °C and 450 °C are the temperatures of the phase order–disorder transition of the L1₀-FePd and L1₂-FePd₃ phases, respectively. These temperatures are in good agreement with the temperature of the formation of L1₀-FePd in Fe/Pd multilayers [6] and bilayers [5,12]. However, they are lower than the temperatures of ordering in FePd (550 °C) and FePd₃ (620 °C) bulk samples [23]. The difference in the order–disorder transition temperatures of film and bulk samples may be related size effects similar to those known to occur in nanoparticles [24].

4. Conclusion

Thus, we investigated phase transformations in epitaxial Pd(0 0 1)/Fe(0 0 1) bilayers with compositions of 1:3 (Fe:Pd) at annealing temperatures up to 650 °C. The successive formation of L1₀-FePd and L1₂-FePd₃ ordered phases at respective temperatures of 400 °C and 450 °C was observed. The L1₂-FePd₃(001) [1 0 0] || MgO(0 0 1)[1 0 0] epitaxial orientation relationship was identified. Unlike FePd, FePd₃ has a magnetically soft phase with low values in its first magnetocrystallographic anisotropy constant ($K_1 = -2.0 \times 10^3$ erg/cm³) and coercivity ($H_C < 1$ Oe).

Acknowledgments

This study was supported by the Analytical Departmental Target Program: Development of Scientific Potential of Higher School 2009–2011, Project no. 2.1.1/9193.

References

- [1] O. Heszko, A. Soroka, S.P. Hannula, Applied Physics Letters 93 (2008) 022503.
- [2] J. Buschbeck, S. Hamann, A. Ludwig, B. Holzapfel, L. Schultz, S. Fähler, Journal of Applied Physics 107 (2010) 113919.
- [3] C. Clavero, J.R. Skuza, Y. Choi, D. Haskel, J.M. Garcia-Martin, A. Cebollada, R.A. Lukaszew, Applied Physics Letters 92 (2008) 162502.
- [4] D. Halley, B. Gilles, P. Bayle-Guillemaud, R. Arenal, A. Marty, G. Patrat, Y. Samson, Physical Review B 70 (2004) 174437.
- [5] A. Kovács, K. Sato, Y. Hirotsu, Journal of Applied Physics 102 (2007) 123512.
- [6] D.H. Wei, Y.D. Yao, Applied Physics Letters 95 (2009) 172503.
- [7] H. Bernas, J.-Ph. Attané, K.-H. Heinig, D. Halley, D. Ravelosona, A. Marty, P. Auric, C. Chappert, Y. Samson, Physical Review Letters 91 (2003) 077203.
- [8] K. Sato, J.G. Wen, J.M. Zuo, Journal of Applied Physics 105 (2009) 093509.
- [9] S. Farjami, T. Fukuda, T. Kakeshita, Journal of Physics: Conference Series 165 (2009) 012055.
- [10] J. Lyubina, O. Gutfleisch, O. Isnard, Journal of Applied Physics 105 (2009) 07A717.
- [11] D. Pečko, K. Žužek Rožman, P.J. McGuinness, B. Pihlar, S. Kobe, Journal of Applied Physics 107 (2010) 09A712.
- [12] V.G. Myagkov, V.S. Zhigalov, L.E. Bykova, L.A. Solov'ev, G.N. Bondarenko, JETP Lett 91 (2010) 481.
- [13] B.A. Belyaev, A.V. Izotov, A.A. Leksikov, IEEE Sensors 5 (2005) 260.
- [14] K. Noda, M. Higuchi, Y. Komaki, T. Tanaka, Y. Nozaki, K. Matsuyama, Journal of Physics: Conference Series 266 (2011) 012014.
- [15] G. Chen, J.X. Li, J. Zhu, J.H. Liang, Y.Z. Wu, Journal of Applied Physics 109 (2011) 07C108.
- [16] F. Cebollada, A. Hernando-Mañeru, A. Hernando, C. Martínez-Boubeta, A. Cebollada, J.M. González, Physical Review B 66 (2002) 174410.
- [17] R. Pretorius, C.C. Theron, A. Vantomme, J.W. Mayer, Critical Reviews in Solid State Materials Science 24 (1999) 1.
- [18] S. Zhang, M. Östling, Critical Review in Solid State Material Science 28 (2003) 1.
- [19] V.G. Myagkov, L.E. Bykova, G.N. Bondarenko, V.S. Zhigalov, A.I. Pol'skiĭ, F.V. Myagkov, JETP Letters 71 (2000) 183.
- [20] V.G. Myagkov, L.A. Li, L.E. Bykova, I.A. Turpanov, P.D. Kim, G.V. Bondarenko, G.N. Bondarenko, Physics Solid State 42 (2000) 968.
- [21] V.G. Myagkov, V.S. Zhigalov, L.E. Bykova, G.N. Bondarenko, Journal of Magnetism and Magnetic Materials 305 (2009) 534.
- [22] V.G. Myagkov, O.A. Bayukov, L.E. Bykova, G.N. Bondarenko, Journal of Magnetism and Magnetic Materials 321 (2009) 2260.
- [23] G. Longworth, Physical Review 172 (1968) 572.
- [24] D. Alloyeau, C. Ricolleau, C. Mottet, T. Oikawa, C. Langlois, Y. Le Bouar, N. Braidı, A. Loiseau, Nature Materials 8 (2009) 940.